

Delayed onset and fast rise of prompt optical-UV emission from gamma-ray bursts in molecular clouds *

Xiao-Hong Cui¹, Zhuo Li^{2,3} and Li-Ping Xin¹

¹ National Astronomical Observatories, Chinese Academy of Sciences, Beijing 100012, China;
xhcui@bao.ac.cn

² Department of Astronomy, Peking University, Beijing 100871, China

³ Kavli Institute for Astronomy and Astrophysics, Peking University, Beijing 100871, China

Received 2012 August 15; accepted 2012 September 2

Abstract Observations imply that long γ -ray bursts (GRBs) originate from the explosions of massive stars, therefore they may occur in the molecular clouds where their progenitors were born. We show that the prompt optical-UV emission from GRBs may be delayed due to dust extinction, which can explain the observed optical delayed onset and fast rise in GRB 080319B well. The density and the size of the molecular cloud around GRB 080319B are roughly constrained to be $\sim 10^3 \text{ cm}^{-3}$ and $\sim 8 \text{ pc}$, respectively. We also investigate other GRBs with prompt optical-UV data, and find similar values of the densities and sizes of the local molecular clouds. Future observations of prompt optical-UV emission from GRBs on a timescale of subseconds, e.g. by UFFO-Pathfinder and SVOM-GWAC, will provide more evidence and probes of the local environments of GRBs.

Key words: radiation mechanisms: non-thermal — gamma-rays: bursts — dust: extinction

1 INTRODUCTION

The properties of a γ -ray burst (GRB) circumburst and the associated host-galaxy environment are important for the studies of GRB progenitors and the fundamental conditions required within a galaxy to form a GRB. The multi-wavelength observations about the emission from GRBs and that from their host galaxies would provide a unique tool to understand the nature of GRBs and the properties of the interstellar medium (ISM) around the bursts.

Observations imply that long GRBs originate from explosions of massive stars. First, they are observed to lie in star-forming galaxies, or even within the active star-forming regions of the host galaxies (e.g. Paczynski 1998; Bloom et al. 2002). More precise HST images of afterglows reveal that they occur within a few kiloparsecs of the flux-weighted centroid of their host galaxies (Fruchter et al. 2006). Second, X-ray observations show evidence for high column densities of gas around long GRBs, implying there are giant molecular clouds around them (e.g. Galama & Wijers 2001). Finally, at least some long GRBs are associated with core-collapse supernovae (SNe). The discovery of four clear associations between long, soft GRBs and Type Ib/c SNe, as well as the appearance of many

* Supported by the National Natural Science Foundation of China.

SN-like bumps in the late optical afterglow light curves (see, e.g., the review by Woosley & Bloom 2006) directly indicates that their progenitors are massive stars.

Because the progenitors of long GRBs are massive stars, they may occur in the birthplace of the progenitors since massive stars are short-lived, i.e. long GRBs may lie in the molecular clouds where the massive stars are born. The optical-UV and X-ray emission from GRBs can be significantly affected by the extinction of dust and absorption of gas in the local environment. However, γ -ray emission is almost unaffected. Therefore, one may naturally expect that the behavior of prompt optical-UV emission is different in light curves from that of prompt γ -ray emission. The difference may hint at the properties of the dust environments around the GRBs. The interaction of a GRB with the environment can yield powerful clues about the properties of the medium in which the burst occurs. The behaviors of the X-ray and optical opacities in the vicinity of a GRB have been studied (Perna et al. 2000; Perna & Raymond 2000). A time-dependent photoionization code has been developed to study the modifications in the dust distribution, and the graphite in the medium around the GRB was found to be more resistant than silicates (Perna & Lazzati 2002; Lazzati & Perna 2002).

The varieties of observed GRB prompt optical behaviors are rich. The prompt optical emission was first observed in GRB 990123 and was found to be uncorrelated with the ongoing γ -ray emission (Akerlof et al. 1999; but see Liang et al. 1999). Then the prompt optical emission from GRB 050820A (Vestrand et al. 2006) was reported and a strong correlation between γ -energy and optical emission in the prompt phase was discovered. Similar cases of some degree of correlation were observed in GRB 041219A (Vestrand et al. 2005; Blake et al. 2005), GRB 060526 (Thöne et al. 2010) and “naked eye” burst GRB 080319B (Racusin et al. 2008; Beskin et al. 2010). GRB 080319B, with the most data from prompt optical observations, has attracted much attention regarding its nature. The detailed observation of this burst presented by Racusin et al. (2008) showed not only a correlation between γ -ray and optical emission in the prompt phase but also an obvious delayed onset of ~ 15 s between them.

In this work, we show that if a GRB is located in a molecular cloud, its prompt optical-UV emission may be absorbed by the dust in the molecular cloud, and only emerges after the dust along the line of sight is completely destroyed. This can explain the observed delayed onset of the prompt optical-UV emission in GRB 080319B well, and the density and size of the molecular cloud around this burst can be roughly constrained. For other bursts with prompt optical observations, the properties of the local environment can also be constrained. We find similar properties of the clouds, with density and size being $n_{\text{H}} \sim 10^3 - 10^4 \text{ cm}^{-3}$ and $\Delta R \sim 6 \text{ pc}$ respectively. The paper is arranged as follows: a simple model of the radiation-dust interaction and the resulting prompt optical-UV light curve are presented in Section 2; in Section 3, we apply the model to GRB 080319B and other GRBs with prompt optical-UV observations; in Section 4 discussion and conclusions are presented.

2 RADIATION-DUST INTERACTION AND EMERGENT OPTICAL-UV EMISSION

Consider a GRB that is located in a molecular cloud. The prompt optical-UV emission from this GRB may be absorbed by the dust in the cloud, but at the same time the dust may also be destroyed by the emission. If the optical-UV emission is strong and lasts long enough, it may emerge from the cloud after the dust along the line of sight path is completely destroyed. The dust destruction by the optical-UV radiation has been discussed by Waxman & Draine (2000). Here we will follow their model in the radiation-dust interaction, and focus on the back effect of the dust on the optical-UV emission, i.e. how the dust in a cloud of finite size affects the apparent light curve of the prompt optical-UV emission. On the other hand, from the observed light curve profile of the prompt optical-UV emission, we can also give some constraints on the properties of the molecular cloud. We will only consider dust destruction due to thermal sublimation and neglect the effect of grain charging,

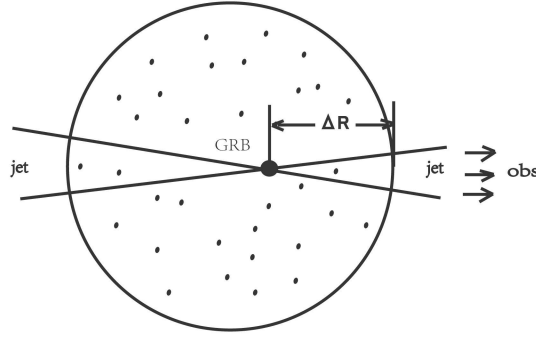


Fig. 1 The sketch of an observed GRB located inside a molecular cloud. “obs” denotes the direction to the Earth (observer). The cloud is assumed to have uniform density and a clear boundary. The distance of the GRB to the edge of the cloud is ΔR , as marked.

since, as argued by Waxman & Draine (2000) and Draine & Hao (2002), the thermal sublimation is likely to be more effective (see, however, Fruchter et al. 2001).

Considering a simple picture as shown in Figure 1, the molecular cloud is assumed to be uniform in density, and the distance of the GRB from the edge of the cloud on the side to the observer is ΔR . The cloud contains dust grains of characteristic radius a and dust number density n_d . Assuming a standard dust-to-gas mass ratio, n_d is related to the cloud density n_H as $n_d = 0.01n_H m_H / (4\pi/3)a^3 \rho$, where ρ is the mass density of the grain material. A characteristic value of $\rho = 3.5 \text{ g cm}^{-3}$ (Guhathakurta & Draine 1989) will be taken in the following calculations. Because the source emits radiation of $1 - 7.5 \text{ eV}$ with luminosity $L_{1-7.5}$, a grain at a distance r can be heated, leading to thermal sublimation and thermal emission. The temperature T of the grain at distance r from the source is governed by

$$\frac{L_{1-7.5}}{4\pi r^2} Q_{UV} \pi a^2 = \langle Q \rangle_T 4\pi a^2 \sigma T^4 - 4\pi a^2 \frac{da}{dt} \frac{\rho}{m} B, \quad (1)$$

where m is the mean atomic mass, B is the chemical binding energy per atom, Q_{UV} is the absorption efficiency factor averaged over the $1 - 7.5 \text{ eV}$ spectrum of the source emission and $\langle Q \rangle_T$ is the usual Planck-averaged absorption efficiency. We will assume $Q_{UV} \approx 1$ for $a \gtrsim 10^{-5} \text{ cm}$ and approximate $\langle Q \rangle_T$ by

$$\langle Q \rangle_T \approx \frac{0.1 a_{-5} (T/2300 \text{ K})}{1 + 0.1 a_{-5} (T/2003 \text{ K})} \quad (2)$$

with $a_{-5} = a/10^{-5} \text{ cm}$. The thermal sublimation rate can be approximated by (Guhathakurta & Draine 1989)

$$\frac{da}{dt} = - \left(\frac{m}{\rho} \right)^{1/3} \nu_0 e^{-B/kT}. \quad (3)$$

We adopt the frequency $\nu_0 = 1 \times 10^{15} \text{ s}^{-1}$, $B/k = 7 \times 10^4 \text{ K}$ and $\rho/m = 10^{23} \text{ cm}^{-3}$ as representative values (Guhathakurta & Draine 1989; Waxman & Draine 2000). If we assume T is approximately constant during the illumination, then the grain survival time at T is $t_{\text{surv}}(T) = a/|da/dt|$. The grain will be completely destroyed by thermal sublimation if it is illuminated over a time longer than $t_{\text{surv}}(T)$.

As the dust is destroyed by the radiation, the radiation is also extinguished by the dust. We can now consider the effects of dust extinction on the observed light curves from the flash. Following

Waxman & Draine (2000), let us approximate the 1–7.5 eV emission from the GRB as a rectangular pulse of duration Δt and luminosity $L_{1-7.5}$. The problem can be simplified by assuming that the effects of extinction can be approximated as a narrowing of the optical pulse, retaining a rectangular profile. The leading edge of the radiation is just at the dust destruction front. We assume that there is a sharp disruption front within which the dust grains are all destroyed, whereas the grains further away are not affected. We define $f(r)$ as the fraction of the flash energy that is absorbed by the dust interior to radius r . If $t_{\text{surv}} < (1 - f)\Delta t$, the grains are destroyed and $f(r)$ satisfies

$$\frac{df}{dr} = Q_{\text{UV}} n_{\text{d}} \pi a^2 \frac{t_{\text{surv}}}{\Delta t}. \quad (4)$$

The relation between the radius of dust destruction front R_f and observer time t_{obs} can be given by

$$t_{\text{obs}} = f(R_f) \Delta t (1 + z), \quad (5)$$

with z being the redshift of the GRB source. A (maximum) dust destruction radius R_{d} is determined by the condition $t_{\text{surv}}[T(R_{\text{d}})] = [1 - f(R_{\text{d}})] \Delta t$. At $r > R_{\text{d}}$, the dust grain survives the illumination and the destruction front does not move any more, therefore we can simply assume $R_f = R_{\text{d}}$ and $f = 1$ at $t_{\text{obs}} > f(R_{\text{d}}) \Delta t (1 + z)$.

The above discussion on propagation of R_f omits the existence of the edge of the cloud at ΔR . If $R_f < \Delta R$, the optical depth due to dust extinction is

$$\tau = Q_{\text{UV}} n_{\text{d}} \pi a^2 (\Delta R - R_f), \quad (6)$$

and the attenuated luminosity observed outside is

$$L_{\text{obs}}(t_{\text{obs}}) = L_{1-7.5} \exp\{-\tau[R_f(t_{\text{obs}})]\}. \quad (7)$$

If $R_{\text{d}} > \Delta R$ then the destruction front can reach the edge ($R_f = \Delta R$) at time $t_{\text{obs}} = f(\Delta R) \Delta t (1 + z)$, which means all the dust in the beam of the radiation is cleared and the radiation is not attenuated, so $\tau = 0$. However, if $R_{\text{d}} < \Delta R$ then the dust is not completely destroyed, and the disruption front stays at R_{d} for $t_{\text{obs}} > f(R_{\text{d}}) \Delta t (1 + z)$ while the dust optical depth is fixed at $\tau = Q_{\text{UV}} n_{\text{d}} \pi a^2 (\Delta R - R_{\text{d}})$.

Note, in the former case where $R_{\text{d}} > \Delta R$, the 1–7.5 eV emission is first totally attenuated, since $R_f < \Delta R$ and $\tau \gg 1$; when the destruction front propagates close to the edge of the cloud, where $R_f \lesssim \Delta R$ and $\tau \sim 1$, some fraction of it starts to emerge; after the destruction front reaches the edge, where $R_f = \Delta R$, the emission emerges completely without any extinction. Thus, the increase in duration for the light curve depends on the edge of cloud ΔR , while the slope of the increasing light curve depends on the propagation speed of the destruction front which is sensitive to the cloud density, n_{H} .

3 APPLICATIONS

As discussed above, in the case of $R_{\text{d}} > \Delta R$, the radiation-dust interaction leads to the case where only the later part of the prompt optical-UV photons emerges, but the γ -ray photons from the GRB have no attenuation. Thus, if the prompt γ -ray and optical-UV radiation is emitted together from the GRB source, there should be a time delay between the onset of the apparent prompt optical-UV and γ -ray emission. So far there are quite a few GRBs that have been detected with prompt optical-UV emission. We will apply the simple radiation-dust interaction model to all these detected GRBs, with the goal of explaining the time delays of the prompt optical-UV emission relative to γ -ray emission, and roughly give some implications to the properties, e.g. the densities and the sizes of the molecular clouds around them.

The observed luminosity is usually given in a single band for a single filter, e.g. U , B , V , R bands, etc. A spectrum with the form $f_\nu \propto \nu^{-1}$ is assumed for the prompt optical-UV flash in 1–7.5 eV, which is consistent with the fast-cooling electrons expected in the standard internal shock model. Thus, a cosmological κ -correction factor can be defined to account for the transformation of the single passband of the filter to the band of 1–7.5 eV in the proper GRB frame,

$$\kappa = \frac{\int_{1\text{eV}/h(1+z)}^{7.5\text{eV}/h(1+z)} f_\nu d\nu}{\int_{b_1}^{b_2} f_\nu d\nu} \quad (8)$$

where b_2 and b_1 are the frequency boundaries of the passband for the observed filter; z is the GRB redshift.

3.1 GRB 080319B

So far, the so-called “naked-eye” GRB 080319B has been the only case that happened to occur in the field of view of an optical telescope, without being triggered by a high-energy detector, thus it was by luck being monitored in the optical band before the beginning of the GRB. The broad-band observations of it were presented by Racusin et al. (2008) and Beskin et al. (2010). The γ -ray emission was found to begin at about 4 s before the BAT trigger and last ~ 57 s. The bright optical transient begins at ~ 10 s after the BAT trigger, peaks at ~ 18 s and then fades below the threshold to magnitude ~ 12 after 5 min. That is to say, there is a time delay of ~ 14 s between the onsets of γ -ray and optical emission. It should be noticed that the optical rise is too fast to be accounted for by the afterglow model, including either forward shock emission (Sari et al. 1998) or reverse shock emission (Kobayashi 2000). The optical light curve during the plateau phase shows fluctuation, similar to the γ -ray one. Moreover, the optical and γ -ray emission is found to be correlated. All these features suggest that the prompt optical emission from this burst is not produced by an afterglow shock. Thus the delayed rising optical emission needs another explanation. We show below that the delay can be explained well by the radiation-dust interaction.

We, again, approximate the intrinsic optical-UV emission as a rectangular pulse of duration Δt (in the rest frame of the GRB). Since the optical emission is observed to decay at ≈ 50 s (similar to the γ -ray duration), the duration is $\Delta t \approx 50/(1+z) \approx 25$ s, where the GRB redshift is $z = 0.937$ (Vreeswijk et al. 2008). Apparently in observations, the optical flux rises from zero to a plateau phase at a time $t_b \approx 15$ s after the trigger, and the plateau phase ends at ~ 50 s. The mean luminosity after t_b (i.e. in the range of 15–50 s) and in the 1–7.5 eV energy band can be given by

$$L_{1-7.5} = 4\pi D_L(z)^2 \kappa f_p \approx 2.6 \times 10^{50} \text{ erg s}^{-1}.$$

Here $D_L(z)$ is the calculated luminosity distance (adopting a Universe model with $\Omega_M = 0.3$, $\Omega_\Lambda = 0.7$ and $H_0 = 71 \text{ km s}^{-1} \text{ Mpc}^{-1}$), and $f_p = 9.39 \times 10^{-9} \text{ erg cm}^{-2} \text{ s}^{-1}$ is the mean flux observed during the time range of 15–50 s in the V band observed by TORTORA (Pagani et al. 2008; Racusin et al. 2008). The correction factor $\kappa = 6.17$ for this burst is calculated by assuming a power law spectrum $f_\nu \sim \nu^{-1}$.

If the duration of the optical-UV emission is taken to be $\Delta t = 25$ s and assuming the radius of a dust grain to be $a = 1 \times 10^{-5} \text{ cm}$, we can calculate the absorbed energy fraction $f(r)$ of the flash up to the destruction radius R_d for a range of cloud densities of $n_H = 10^2 - 10^5 \text{ cm}^{-3}$. The result is shown in Figure 2. We can see that the denser the cloud, the faster the flash energy is absorbed. However, after the destruction front reaches the destruction radius $r = R_d$, the absorbed fraction rapidly reaches unity, $f(R_d) = 1$.

As is apparent in observations, the optical emission rises to the mean flux level at about 15 s, and then maintains this level until ~ 50 s. This implies that the absorbed fraction of the flash energy, when the dust destruction front reaches the edge of the cloud, is $f(R_f = \Delta R) \approx 15/50 = 0.3$. Thus, given

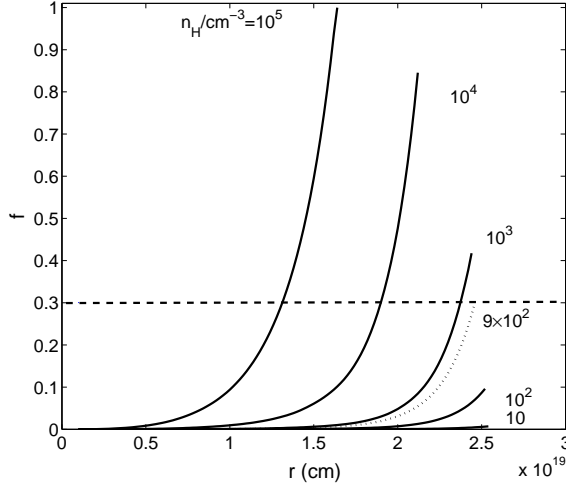


Fig. 2 The fraction $f(r)$ of flash energy absorbed by the dust interior to radius r up to dust destruction radius $r = R_d$ in the case of GRB 080319B. The duration and luminosity of prompt emission in 1–7.5 eV are $\Delta t = 25$ s and $L_{1-7.5} = 2.6 \times 10^{50}$ erg s^{-1} , respectively, and the dust grain size is assumed to be $a = 10^{-5}$ cm. Different lines correspond to different values of cloud density n_H , as marked in the plot. The dashed line shows $f(r = \Delta R) = 0.3$. The dotted line presents the case of $f(r = R_d) = 0.3$, i.e. $R_d = \Delta R$.

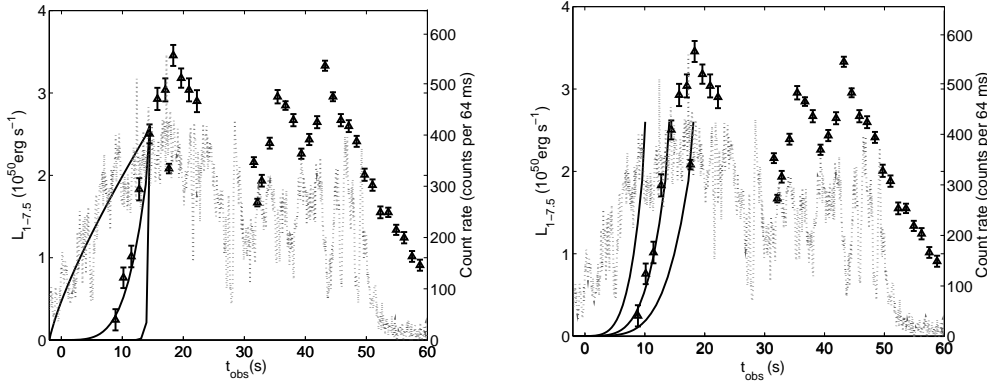


Fig. 3 The light curves of GRB 080319B in γ -ray and optical bands. The black triangles are optical data from TORTORA. For comparison, the γ -ray light curve (18–1160 keV) that has the Konus-Wind background subtracted, with respect to the trigger time by Swift-BAT, is shown as a dotted line. The solid lines are the calculated optical light curves in the simple radiation-dust interaction model. *Left panel:* The cases with the cloud density $n_H = 10^2, 10^3$ and 10^4 cm^{-3} (corresponding to three light curves from left to right respectively) and the fixed end time of the rising part $t_b = 16$ s. *Right panel:* The cases with $t_b = 12, 16$ and 20 s (from left to right respectively) and fixed $n_H = 10^3$ cm^{-3} . The other parameters are the same as in Figure 2. The case with $t_b = 16$ s and $n_H = 10^3$ cm^{-3} gives the best fit to the rising part of the optical flash of GRB 080319B.

the cloud density n_{H} , the cloud's size, roughly indicated by ΔR , can be determined for this burst, i.e. n_{H} and ΔR are related for a fixed value of $f(r = \Delta R)$. For example, if $n_{\text{H}} = (10^3, 10^4, 10^5) \text{ cm}^{-3}$, we have $\Delta R = (2.4, 1.7, 1.1) \times 10^{19} \text{ cm}$, respectively, with fixed $f(r = \Delta R) = 0.3$. Then the value of ΔR can be found to decrease with a larger value of n_{H} . However, for too small n_{H} , the destruction front reaches the maximum destruction radius R_{d} before arriving at the edge of the cloud, i.e. the absorbed fraction $f(r = R_{\text{d}}) < 0.3$, as in the case of $n_{\text{H}} = 10^2 \text{ cm}^{-3}$ in Figure 2.

In order to decouple n_{H} and ΔR , we need to further consider the temporal profile of the observed optical-UV emission. For different values of n_{H} and t_{b} , we have calculated the optical-UV light curve using Equation (7). The resulting light curves are shown in Figure 3; also plotted are the γ -ray and optical-UV data that are adopted from Racusin et al. (2008). Note, as Beskin et al. (2010) found that the optical emission is delayed 2 s relative to the γ -ray emission in the plateau phase, we also assume a time delay of 2 s for the intrinsic onset of optical-UV emission compared to the γ -ray one. The plotted light curves in Figure 3 take this into account. We see that compared with the observed optical data of GRB 080319B, the case with $n_{\text{H}} = 10^3 \text{ cm}^{-3}$ and $t_{\text{b}} = 16 \text{ s}$ fits the light curve profile better. Therefore, it can be concluded that the cloud that hosts GRB 080319B has a density of $n_{\text{H}} \approx 10^3 \text{ cm}^{-3}$ and a size of $R \sim \Delta R \approx 8 \text{ pc}$.

It should be noted that in the above calculations we have taken $\rho = 3.5 \text{ g cm}^{-3}$ (Guhathakurta & Draine 1989), $a = 1 \times 10^{-5} \text{ cm}$ and a standard dust-to-gas mass ratio of 0.01. The resulting values of n_{H} , ΔR and R_{d} are not sensitive to these values, i.e. the resulting n_{H} , ΔR and R_{d} values vary within a factor of a few if ρ , a , κ and the gas-to-dust ratio change by one order of magnitude. This is good enough for order of magnitude estimates using the simple model given here.

3.2 Other GRBs with Prompt Optical Detections

Besides GRB 080319B, there are quite a few other GRBs with prompt optical detections during the γ -ray bursting phase. They have all been detected by a rapid slew of optical telescopes to the location of the GRB after being triggered by γ -ray detectors. So usually there is a gap between the trigger time and the start time of optical observation. Nevertheless, we can still try to make some constraints on the local GRB environments based on the simple radiation-dust interaction model.

All the GRBs detected after December of 2004 which have optical detections during the prompt γ -ray emission are collected and analyzed with the simple radiation-dust interaction model described here. We separate these GRBs into two samples. In *Sample I*, the GRBs satisfy the following three criteria: (1) there are optical detections before the end of the GRB, specifically, the optical detection is within the duration of T_{90} ; (2) the optical light curve within T_{90} shows a rise in the flux, i.e. if the optical light curve shows a decay or flat plateau then the GRB is not included; (3) the number of optical data points, excluding upper limits, in the rising part is not less than three. All the other GRBs only satisfy criterion (1) and are grouped into *Sample II*.

We find that besides GRB 080319B, there are seven other GRBs that satisfy the three criteria: GRB 041219A (Vestrand et al. 2005; Blake et al. 2005); GRB 050820A (Vestrand et al. 2006); GRB 060218 (Mirabal et al. 2006; Ferrero et al. 2006; Sollerman et al. 2006; Kocevski et al. 2007); GRB 060418 (Molinari et al. 2007; Dupree et al. 2006; Vreeswijk & Jaunsen 2006); GRB 060607A (Molinari et al. 2007; Ledoux et al. 2006); GRB 080810 (Page et al. 2009; Burenin et al. 2008) and GRB 100906A (Gorbovskoy et al. 2012; Barthelmy et al. 2010; Markwardt et al. 2010; Tanvir et al. 2010). However, we exclude GRB 041219A and GRB 060218 from Sample I for the following reasons: GRB 041219A shows a correlation between γ -ray and optical emission, thus the observed initial rise in the optical band is likely intrinsic (Vestrand et al. 2005) instead of due to radiation-dust interaction. This GRB is included in Sample II instead. As for GRB 060218, its early optical-UV emission is likely to be associated with breakout of the supernova shock (Campana et al. 2006; Waxman et al. 2007), and thus also not due to radiation-dust interaction.

Table 1 The Observational Results of GRBs in Sample I and the Constraints of their Local Molecular Clouds

GRB	z	T_{90} (s)	t_{op} (s)	κ^*	$L_{1-7.5}$ ($10^{48} \text{ erg s}^{-1}$)	R_d (pc)	ΔR (pc)	n_{H} (10^3 cm^{-3})	Δt_{obs} (s)	t_b (s)	Reference
050820A	2.6	750 **	84	3.10 (R)	0.6	3.35	3.23	9	646	305	[1, 2, 3]
060418	1.49	103.1	40	4.07 (H)	2.4	6.91	6.87	4	140	107	[4, 5, 6]
060607A	3.082	102	73	4.07 (H)	2.3	5.90	5.87	5	200	150	[4, 7]
080319B	0.937	57	8.9 †	6.17 (V)	260	7.78	7.67	1	50	16	[8, 9, 10]
080810	3.35	106	38	3.10 (W)	7.1	11.7	11.4	3	150	67	[11, 12]
100906A	1.727	114.4	48.5	3.10 (W)	1.2	4.60	4.48	15	190	83	[13, 14, 15, 16]

* In the bracket is the passband of the filter. Letters “V,” “H” and “W” denote the V, H and white bands, respectively.

** From the work of Vestrand et al. (2006), rather than Swift data.

† The time corresponds to the first optical data by TORTORA. In fact, the optical observations start before the trigger of this GRB.

References: [1] Prochaska et al. (2005); [2] Ledoux et al. (2005); [3] Vestrand et al. (2006); [4] Molinari et al. (2007); [5] Dupree et al. (2006); [6] Vreeswijk & Jaunsen (2006); [7] Ledoux et al. (2006); [8] Vreeswijk et al. (2008); [9] Racusin et al. (2008); [10] Beskin et al. (2010); [11] Page et al. (2009); [12] Burenin et al. (2008); [13] Gorbovskoy et al. (2012); [14] Barthelmy et al. (2010); [15] Markwardt et al. (2010); [16] Tanvir et al. (2010).

Table 2 The Observational Results of GRBs in Sample II and the Constraints of their Local Molecular Clouds

GRB	z	T_{90} (s)	t_{op} (s)	$L_{1-7.5}$ ($10^{47} \text{ erg s}^{-1}$)	Reference
041219A	0.31	520	460	3.7×10^{-5}	[1, 2]
050319	3.24	160.5	30.4	3.9	[3, 4]
050904	6.29	174.2	150.3	1.1	[5]
060526	3.21	298.2	16.1	3.4	[6]
060904B	0.703	171.5	21	$< 6.8 \times 10^{-2}$	[7]
061126	1.16	70.8	42	1.9×10^{-2}	[8, 9]
071003	1.1	150	44.5	3.0	[10]
071031	2.69	180	59.6	2.3	[11, 12]
080603A	1.69	150	105	5.8×10^{-3}	[13]
080607	3.036	79	24.5	2.7	[14]
100901A	1.408	439	113.4	9.6×10^{-2}	[15, 16, 17]
100902A	4.5	428.8	104	< 1.4	[17]
110205A	1.98	257	166	0.2	[18]

References: [1] Vestrand et al. (2005); [2] Blake et al. (2005); [3] Quimby et al. (2006); [4] Woźniak et al. (2005); [5] Boër et al. (2006); [6] Thöne et al. (2010); [7] Klotz et al. (2008); [8] Gomboc et al. (2008); [9] Perley et al. (2008a); [10] Perley et al. (2008b); [11] Kruehler et al. (2007); [12] Antonelli et al. (2007); [13] Guidorzi et al. (2011); [14] Perley et al. (2011); [15] Chornock et al. (2010); [16] Immler et al. (2010); [17] Gorbovskoy et al. (2012); [18] Cucchiara et al. (2011).

Sample I GRBs are listed in Table 1. All the other GRBs that only satisfy criterion (1) are grouped into *Sample II*. For example, GRB 110205A (Klotz et al. 2011a,b; Cucchiara et al. 2011) started to be detected in the optical band 166 s after being triggered, but is within the duration of $T_{90} = 257$ s. The observed optical light curve already appears to be a plateau, without a rising part, which may occur before the start of optical detections. We exclude this burst from Sample I but include it in Sample II. As shown in Table 2, there are 13 GRBs in Sample II.

3.2.1 Sample I

For GRBs in Sample I, we can follow the same approach we used for GRB 080319B, and the optical rise can be accounted for by the simple radiation-dust interaction model; at the same time the local environments of these bursts are constrained by fitting the observed prompt optical-UV light curves.

We assume that there is intrinsic optical-UV emission associated with the γ -ray emission, with an approximately rectangular light curve profile. The optical-UV duration $\Delta t_{\text{obs}} = \Delta t(1+z)$ is obtained from observations (which is usually comparable or somewhat larger than the γ -ray duration). The luminosity $L_{1-7.5}$ is calculated from observed optical emission, by correction with κ factor assuming an $f_\nu \propto \nu^{-1}$ spectrum (for the white band the same κ factor as the R band is assumed). There are usually fluctuations of optical flux in the plateau phase, thus we use the average of optical flux during the plateau phase (i.e. after the rising part and before the decay phase) to calculate the $L_{1-7.5}$ values: We average the optical data of GRB 050820A during the period of $t_{\text{obs}} = 230 - 722$ s; GRB 060418 of $107 - 137$ s; GRB 060607A of $159 - 205$ s; GRB 080810 of $67 - 261$ s; and for GRB 100906A we use the peak flux at 115 s.

Given $L_{1-7.5}$ and Δt , the maximum dust destruction radius R_d can be determined to be a function of density n_H . Furthermore, the time t_b that the optical flux rises to the top value can be estimated from the observed optical light curve. Once given $f(r = \Delta R) = t_b/\Delta t_{\text{obs}}$ and combined with the condition of $R_d = \Delta R$, one obtains a minimum n_H value, $n_H > n_{H,0}$, otherwise, the destruction front cannot reach the edge of the cloud and no optical-UV emission escapes from the cloud. Finally, we apply Equation (7) to fit the rising part of the optical light curve by taking n_H (in the range of $n_H > n_{H,0}$) and t_b as free parameters. The best fit gives us the resulting values of n_H and ΔR .

The resulting values of n_H and ΔR are also listed in Table 1. Illustrations of our fitting results for the four bursts included in Sample I are shown in Figure 4. From the fitting results, we find that the density of the surrounding molecular clouds are in the range of $10^3 - 10^4 \text{ cm}^{-3}$, while the size, as indicated by ΔR , is on the order of ~ 10 pc. However, due to a small number of GRBs with an optical rising part detected in prompt emission, it is impossible to give the statistical discussion of the properties of local molecular clouds. Furthermore, the observed data points in the optical rising part are usually sparse for an individual GRB, which may induce large errors in light curve fitting. In the future, precise observations are needed to test the model and constrain the properties of the local environment more precisely.

3.2.2 Sample II

For GRBs in Sample II, because there is no optical rise detected due to the delay of optical observations, we cannot well constrain the properties of the surrounding environments. However we still try to make some constraints, although they are rough. In these bursts, the time t_b when the optical-UV flux reaches the plateau, i.e. when the dust destruction front reaches the edge of the cloud, $R_f = \Delta R$, can be considered to be smaller than the start time of the optical observations, t_{op} . Thus we have $t_b < t_{\text{op}}$. Moreover, we take the flux of the first optical data point to calculate the mean luminosity in the optical-UV band. In these bursts, the maximum dust destruction radius must be within the boundary of the cloud, $R_d < \Delta R$, otherwise the optical emission from these GRBs cannot emerge.

Thus we constrain the properties of the molecular clouds of sample-II GRBs as follows. Considering an optical-UV flash with luminosity $L_{1-7.5}$ and duration $\Delta t = t_{\text{op}}/(1+z)$, we can calculate the maximal dust destruction radius as a function of the surrounding density. This puts an upper limit on the value of ΔR of the relevant GRB. The results for all GRBs in Sample II are shown in Figure 5. We see that although there are no good constraints on density n_H , the value of ΔR is quite well constrained since ΔR does not vary much with n_H . All cases except GRB 041219A have upper limits of $\Delta R < 0.1 - 2$ pc, somewhat less than those of sample-I GRBs. This might be reason-

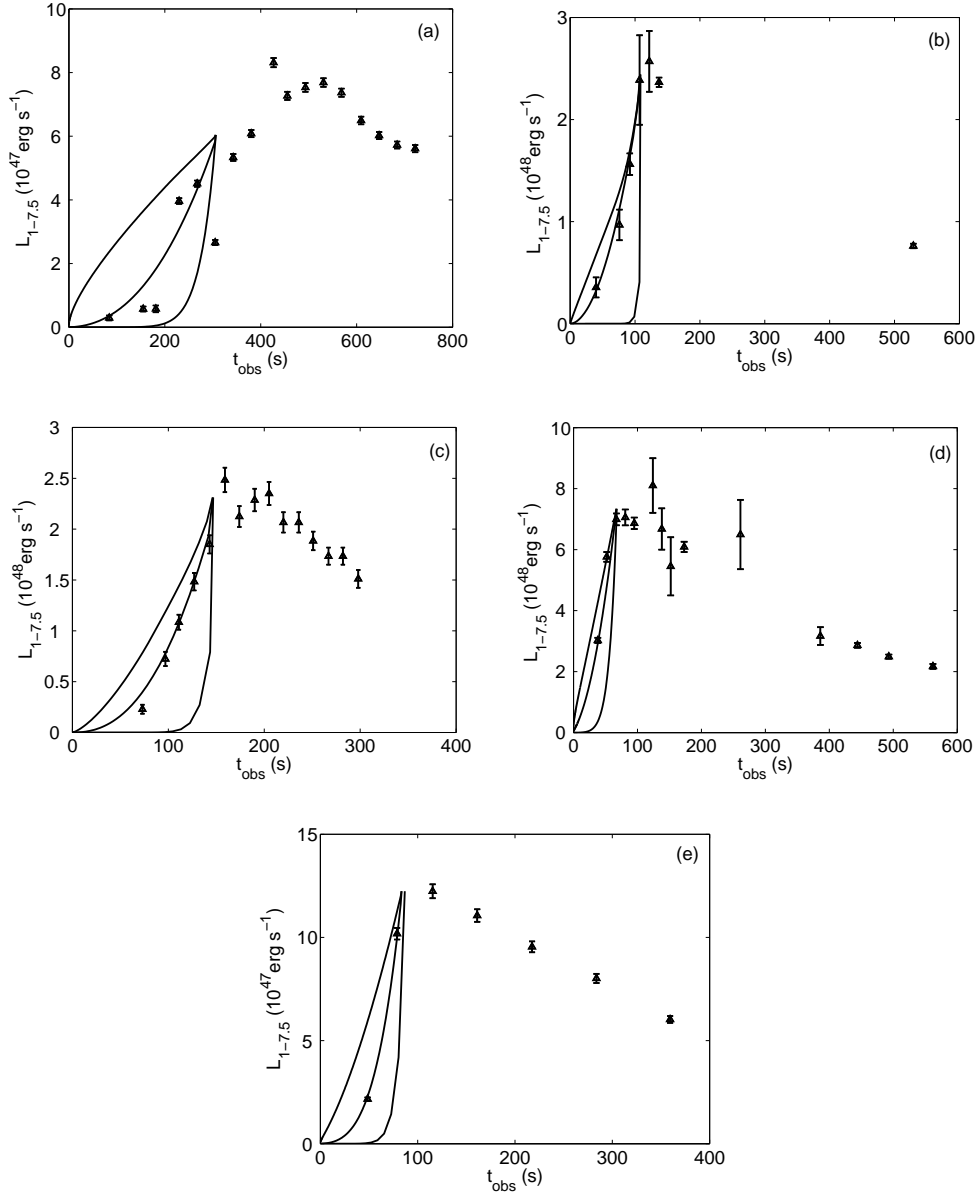


Fig. 4 The light curves of prompt optical emission from five other GRBs in Sample I besides GRB 080319B. The name and the parameters (n_H and t_b) for the fittings are as follows. (a) GRB 050820A: $t_b = 305$ s, $n_H = 3 \times 10^3, 9 \times 10^3, 5 \times 10^4$ cm $^{-3}$; (b) GRB 060418: $t_b = 107$ s, $n_H = 3 \times 10^3, 4 \times 10^3, 5 \times 10^4$ cm $^{-3}$; (c) GRB 060607A: $t_b = 150$ s, $n_H = 3 \times 10^3, 5 \times 10^3, 3 \times 10^4$ cm $^{-3}$; (d) GRB 080810: $t_b = 67$ s, $n_H = 2 \times 10^3, 3 \times 10^3, 3 \times 10^4$ cm $^{-3}$; (e) GRB 100906A: $t_b = 83$ s, $n_H = 6 \times 10^3, 1.5 \times 10^4, 3 \times 10^5$ cm $^{-3}$. The black triangles are the optical data. The solid lines are the predictions from radiation-dust interaction model.

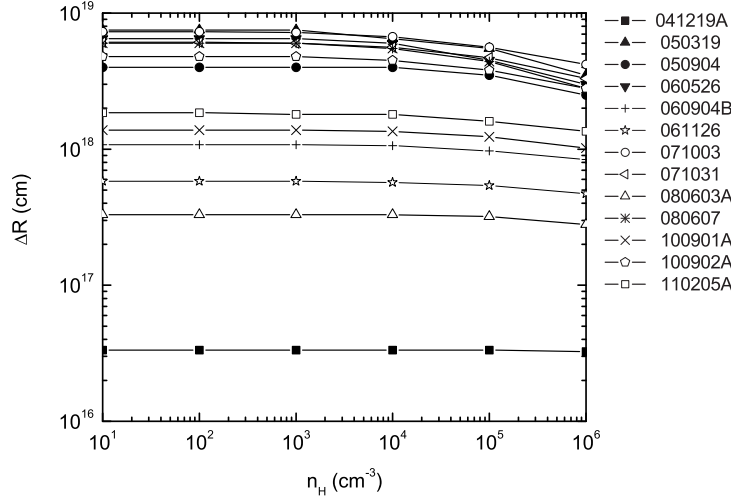


Fig. 5 The constraints on the sizes and densities of molecular clouds around GRBs in Sample II. The region of allowed parameters for each GRB is below the line corresponding to it.

able since the luminosities of sample-II GRBs are generally smaller than those of sample-I GRBs. GRB 041219A has an exceptionally small luminosity; its value of ΔR is smaller than ~ 0.01 pc.

4 DISCUSSION AND CONCLUSIONS

Long GRBs are believed to be the explosions of massive stars, therefore the GRBs may occur in the molecular clouds where their progenitors were born. In this work, we show that the prompt optical-UV emission from GRBs, if originally emitted simultaneously with γ -ray emission, may appear with a relative time delay in observations, due to dust extinction. This can explain the optical delayed onset observed in GRB 080319B well, and the number density and the size of the molecular cloud are roughly constrained to be $n_H \sim 10^3 \text{ cm}^{-3}$ and $\Delta R \sim 8$ pc, respectively. We also investigate the other GRBs with good optical-UV data, and find the densities and sizes of the molecular clouds to be in the range of $n_H \sim 10^3 - 10^4 \text{ cm}^{-3}$ and $\Delta R \sim 10$ pc respectively.

We use a simple picture that the effect of extinction is approximated as a narrowing of the optical pulse, retaining a rectangular profile. This neglects the notion that there may be fluctuation of the original flux with time, and that the dust destruction front does not have zero-thickness. Thus the constraints on the molecular clouds only make sense by order of magnitude.

The resulting n_H and ΔR constraints suggest high column densities of gas around GRBs, $\sim 10^{22} - 10^{23} \text{ cm}^{-2}$. It is interesting to note that Galama & Wijers (2001) obtain a similar range of column densities by observations of X-ray afterglow spectra. Moreover, our constraints are also consistent with those giant molecular clouds found in the Milky Way, which are observed to have sizes of $10 - 30$ pc and average gas densities of $10^2 - 10^3 \text{ cm}^{-3}$ (Winnewisser et al. 1979; Goldsmith 1987). Although the molecular clouds that host GRBs seem, from our constraints, to be slightly denser, the low number of GRBs with prompt optical detection and the sparse data points for individual GRBs prevent us from giving clear conclusions.

One may expect that the initial fast rise of the prompt optical flux can be produced by the afterglow forward shock due to sweep-up of the circumburst medium before deceleration. However, the multi-band observations of two sample-I GRBs 060418 and 060607A show spectral indices in

the optical band of $F_\nu \propto \nu^{-0.9}$ and $F_\nu \propto \nu^{-0.8}$, respectively. This implies the injection frequency is below the optical band, $\nu_m < \nu_{\text{opt}}$, and requires extremely unusual afterglow model parameters, e.g. postshock electron energy far smaller than the typical value, $\epsilon_e \lesssim 10^{-3}$. Moreover, most GRBs in Sample I show increases even faster than $F_\nu \propto t^3$ (e.g. GRBs 060418, 060607A, 080319B and 100906A), which is faster than the model prediction for the pre-deceleration forward shock emission at $\nu > \nu_m$. One may also expect that the rising part can be accounted for by the reverse shock emission due to the process of shock sweeping outflow material, but the predicted temporal slope is not faster than $F_\nu \propto t^2$ (Kobayashi 2000). Thus the prompt optical emission is more likely to be generated within the outflow.

The density of the surroundings from our constraints is higher in general than the medium density indicated by afterglow modeling. The X-ray absorber must lie within 1 – 5 pc from the GRB, thus probing the innermost region in the close vicinity of the GRB explosion. Comparing the HI column densities from Ly α absorption to the metal column densities from X-ray absorption in GRB afterglows, Watson et al. (2007) found that there is no correlation between the column density values, and the X-ray absorptions often far exceed the HI column densities. Based on a detailed study of the absorption pattern, Campana et al. (2011) found a high-metallicity absorbing medium for GRB 090618 in Ne and Si, with best-fitting column densities of $6 \times 10^{17} \text{ cm}^{-2}$. However there is no contradiction here because the size of the observed afterglow is usually on a sub-pc scale, but the region under scrutiny here covers a much larger scale, ~ 10 pc, which results from the constraints. Thus, it may be that in places very close to the GRB’s location, the medium density is low while the regions further-out have much denser gas. This is reasonable because the vicinity of the GRB source may be affected by the progenitor before the GRB explosion.

In our simple model, for given luminosity and duration of the prompt optical-UV emission, the maximum dust destruction radius can be determined. Once it is within the boundary of the cloud, $R_d < \Delta R$, there will neither be prompt optical emission nor optical afterglow emission observed. The GRB will appear optically dark in this case. It is interesting to note that only 60% of GRBs observed by BAT/Swift are detected by UVOT/Swift in the optical afterglows. The “dark bursts” (van der Horst et al. 2009) are still a mystery. If dust extinction is the reason, then by our simple model, this suggests that the maximum dust destruction radii and the sizes of the molecular cloud are statistically comparable, i.e. $R_d \sim \Delta R$, thus the bright and dark bursts are comparable in numbers. Indeed, as shown in Table 1, for those bright GRBs in Sample I with better observations and hence better constraints, R_d and ΔR values are similar.

There are quite a few small robotic telescopes that have been built and installed around the world in order to detect the optical counterparts in the early phase of γ -ray bursts, such as SuperLOTIS (Park & Band 1997), TAROT (Klotz et al. 2009), PROMPT (Reichart et al. 2005), ROTSE-III (Rykoff et al. 2009), SkyNet¹, WIDGET (Urata et al. 2011), MASTER², Pi of the sky (Burd et al. 2005), and TORTORA³, etc. With their large field of view (FOV) and fast slewing abilities, these telescopes are able to detect the prompt optical emission on a timescale of minutes after the trigger of GRBs by γ -ray detectors. In the case of the “naked-eye GRB” 080319B (Racusin et al. 2008), the prompt optical emission was caught by the TORTORA and Pi of the sky even with zero time delay. Besides, the UFFO-Pathfinder (Chen 2011), which aims at prompt optical detection on a timescale of subseconds, will be launched soon; the Ground-based Wide-Angle Camera array (GWAC), with a larger FOV (~ 8000 square degrees), as part of the ground system in the Chinese-French SVOM mission (Paul et al. 2011), aims to search for the optical emission with zero delay, and will be constructed in the near future. All these robotic telescopes and planned projects will compile a larger and better sample of prompt optical emission from GRBs in the future, leading to more precise constraints on the GRB local environments.

¹ <http://skynet.unc.edu/>

² <http://observ.pereplet.ru/>

³ <http://www.eso.org/public/images/eso0808a/>

Acknowledgements We would like to thank the useful discussions with the pulsar group at PKU and with the SVOM group at NAOC. This work is supported by the National Basic Research Program of China (973 Program, 2009CB824800), the China Postdoctoral Science Foundation funded project (No. 20110490590), the National Natural Science Foundation of China (Grant No. 111030262) and the Foundation for the Authors of National Excellent Doctoral Dissertations of China.

References

- Akerlof, C., Balsano, R., Barthelmy, S., et al. 1999, *Nature*, 398, 400
- Antonelli, L. A., Covino, S., D'Avanzo, P., et al. 2007, *GRB Coordinates Network*, 7025, 1
- Barthelmy, S. D., Baumgartner, W. H., Cummings, J. R., et al. 2010, *GRB Coordinates Network*, 11218, 1
- Beskin, G., Karpov, S., Bondar, S., et al. 2010, *ApJ*, 719, L10
- Blake, C. H., Bloom, J. S., Starr, D. L., et al. 2005, *Nature*, 435, 181
- Bloom, J. S., Kulkarni, S. R., & Djorgovski, S. G. 2002, *AJ*, 123, 1111
- Boër, M., Atteia, J. L., Damerdjji, Y., et al. 2006, *ApJ*, 638, L71
- Burd, A., Cwiok, M., Czyrkowski, H., et al. 2005, *New Astron.*, 10, 409
- Burenin, R., Khamitov, I., Galeev, A., et al. 2008, *GRB Coordinates Network*, 8088, 1
- Campana, S., Salvaterra, R., Tagliaferri, G., Kouveliotou, C., & Grindlay, J. 2011, *MNRAS*, 410, 1611
- Campana, S., Mangano, V., Blustin, A. J., et al. 2006, *Nature*, 442, 1008
- Chen, P. 2011, in *International Cosmic Ray Conference*, vol. 8, 240 (arXiv:1106.3929)
- Chornock, R., Berger, E., Fox, D., et al. 2010, *GRB Coordinates Network*, 11164, 1
- Cucchiara, A., Cenko, S. B., Bloom, J. S., et al. 2011, *ApJ*, 743, 154
- Draine, B. T., & Hao, L. 2002, *ApJ*, 569, 780
- Dupree, A. K., Falco, E., Prochaska, J. X., Chen, H.-W., & Bloom, J. S. 2006, *GRB Coordinates Network*, 4969, 1
- Ferrero, P., Kann, D. A., Zeh, A., et al. 2006, *A&A*, 457, 857
- Fruchter, A., Krolik, J. H., & Rhoads, J. E. 2001, *ApJ*, 563, 597
- Fruchter, A. S., Levan, A. J., Strolger, L., et al. 2006, *Nature*, 441, 463
- Galama, T. J., & Wijers, R. A. M. J. 2001, *ApJ*, 549, L209
- Goldsmith, P. F. 1987, in *Interstellar Processes, Astrophysics and Space Science Library*, vol. 134, eds. D. J. Hollenbach & H. A. Thronson, Jr. (Interstellar Processes, Dordrecht: Reidel), 51
- Gomboc, A., Kobayashi, S., Guidorzi, C., et al. 2008, *ApJ*, 687, 443
- Gorbovskey, E. S., Lipunova, G. V., Lipunov, V. M., et al. 2012, *MNRAS*, 421, 1874
- Guhathakurta, P., & Draine, B. T. 1989, *ApJ*, 345, 230
- Guidorzi, C., Kobayashi, S., Perley, D. A., et al. 2011, *MNRAS*, 417, 2124
- Immler, S., Barthelmy, S. D., Baumgartner, W. H., et al. 2010, *GRB Coordinates Network*, 11159, 1
- Klotz, A., Gendre, B., Stratta, G., et al. 2008, *A&A*, 483, 847
- Klotz, A., Boër, M., Atteia, J. L., & Gendre, B. 2009, *AJ*, 137, 4100
- Klotz, A., Gendre, B., Lass, M., Boer, M., & Atteia, J. L. 2011a, *GRB Coordinates Network*, 11630, 1
- Klotz, A., Gendre, B., Lass, M., Boer, M., & Atteia, J. L. 2011b, *GRB Coordinates Network*, 11632, 1
- Kobayashi, S. 2000, *ApJ*, 545, 807
- Kocevski, D., Modjaz, M., Bloom, J. S., et al. 2007, *ApJ*, 663, 1180
- Kruehler, T., Greiner, J., Afonso, P., et al. 2007, *GRB Coordinates Network*, 7021, 1
- Lazzati, D., & Perna, R. 2002, *MNRAS*, 330, 383
- Ledoux, C., Vreeswijk, P., Ellison, S., et al. 2005, *GRB Coordinates Network*, 3860, 1
- Ledoux, C., Vreeswijk, P., Smette, A., Jaunsen, A., & Kaufer, A. 2006, *GRB Coordinates Network*, 5237, 1
- Liang, E. P., Crider, A., Böttcher, M., & Smith, I. A. 1999, *ApJ*, 519, L21
- Markwardt, C. B., Barthelmy, S. D., Beardmore, A. P., et al. 2010, *GRB Coordinates Network*, 11227, 1
- Mirabal, N., Halpern, J. P., An, D., Thorstensen, J. R., & Terndrup, D. M. 2006, *ApJ*, 643, L99

- Molinari, E., Vergani, S. D., Malesani, D., et al. 2007, *A&A*, 469, L13
- Paczynski, B. 1998, *ApJ*, 494, L45
- Pagani, C., Racusin, J. L., Holland, S. T., & Barthelmy, S. D. 2008, GCN Report, 121, 1
- Page, K. L., Willingale, R., Bissaldi, E., et al. 2009, *MNRAS*, 400, 134
- Park, H. S., & Band, D. 1997, NASA STI/Recon Technical Report N, 99, 36147 (arXiv:astro-ph/9711170)
- Paul, J., Wei, J., Basa, S., & Zhang, S.-N. 2011, *Comptes Rendus Physique*, 12, 298
- Perley, D. A., Bloom, J. S., Butler, N. R., et al. 2008a, *ApJ*, 672, 449
- Perley, D. A., Li, W., Chornock, R., et al. 2008b, *ApJ*, 688, 470
- Perley, D. A., Morgan, A. N., Updike, A., et al. 2011, *AJ*, 141, 36
- Perna, R., Raymond, J., & Loeb, A. 2000, *ApJ*, 533, 658
- Perna, R., & Raymond, J. 2000, *ApJ*, 539, 706
- Perna, R., & Lazzati, D. 2002, *ApJ*, 580, 261
- Prochaska, J. X., Bloom, J. S., Wright, J. T., et al. 2005, GRB Coordinates Network, 3833, 1
- Quimby, R. M., Rykoff, E. S., Yost, S. A., et al. 2006, *ApJ*, 640, 402
- Racusin, J. L., Karpov, S. V., Sokolowski, M., et al. 2008, *Nature*, 455, 183
- Reichert, D., Nysewander, M., Moran, J., et al. 2005, *Nuovo Cimento C Geophysics Space Physics C*, 28, 767
- Rykoff, E. S., Aharonian, F., Akerlof, C. W., et al. 2009, *ApJ*, 702, 489
- Sari, R., Piran, T., & Narayan, R. 1998, *ApJ*, 497, L17
- Sollerman, J., Jaunsen, A. O., Fynbo, J. P. U., et al. 2006, *A&A*, 454, 503
- Tanvir, N. R., Wiersema, K., & Levan, A. J. 2010, GRB Coordinates Network, 11230, 1
- Thöne, C. C., Kann, D. A., Jóhannesson, G., et al. 2010, *A&A*, 523, A70
- Urata, Y., Tashiro, M. S., Tamagawa, T., et al. 2011, *PASJ*, 63, 137
- van der Horst, A. J., Kouveliotou, C., Gehrels, N., et al. 2009, *ApJ*, 699, 1087
- Vestrand, W. T., Woźniak, P. R., Wren, J. A., et al. 2005, *Nature*, 435, 178
- Vestrand, W. T., Wren, J. A., Woźniak, P. R., et al. 2006, *Nature*, 442, 172
- Vreeswijk, P., & Jaunsen, A. 2006, GRB Coordinates Network, 4974, 1
- Vreeswijk, P. M., Smette, A., Malesani, D., et al. 2008, GRB Coordinates Network, 7444, 1
- Watson, D., Hjorth, J., Fynbo, J. P. U., et al. 2007, *ApJ*, 660, L101
- Waxman, E., & Draine, B. T. 2000, *ApJ*, 537, 796
- Waxman, E., Mészáros, P., & Campana, S. 2007, *ApJ*, 667, 351
- Winnewisser, G., Churchwell, E., & Walmsley, C. M. 1979, in *Modern Aspects of Microwave Spectroscopy*, ed. G. W. Chantry (London, Academic Press Inc.), 313
- Woodsley, S. E., & Bloom, J. S. 2006, *ARA&A*, 44, 507
- Woźniak, P. R., Vestrand, W. T., Wren, J. A., et al. 2005, *ApJ*, 627, L13